

# Eight-Coordinate Endohedral Rhenium, Osmium and Iridium Atoms in Rare-Earth Halide Cluster Complexes

Sina Zimmermann,<sup>[a]</sup> Matthias Brühmann,<sup>[a]</sup> Frederick Casper,<sup>[b]</sup> Oliver Heyer,<sup>[c]</sup>  
Thomas Lorenz,<sup>[c]</sup> Claudia Felser,<sup>[b]</sup> Anja-Verena Mudring,<sup>\*[d]</sup> and Gerd Meyer<sup>\*[a]</sup>

**Keywords:** Cluster compounds / Crystal structures / Electronic structure / Endohedral atoms

Endohedral (interstitial) atoms are essential for almost all of the rare-earth halide cluster complexes. Most of these contain octahedral clusters, some are isolated, but the majority exhibits condensation by common edges to structures of higher dimensionality. Higher coordination numbers of the endohedral atoms are rare. Four examples of extended cluster complexes with eight-coordinate endohedral atoms of sixth-period elements (Re, Os, Ir) are presented. In the quasi-isostructural, non-isotypic halides {ReGd<sub>4</sub>}Br<sub>4</sub> and {OsSc<sub>4</sub>}Cl<sub>4</sub>, square antiprisms of gadolinium and scandium atoms, respectively, are connected by two common faces to chains, surrounded and loosely connected by halogenido ligands.

The Re and Os atoms build a slightly bent chain with only little bonding interactions. Chemical bonding is dominated by endohedral atom–cluster atom and cluster atom–halide interactions. The same is true for the two scandium bromides {Ir<sub>3</sub>Sc<sub>12</sub>}Br<sub>16</sub> and {Os<sub>3</sub>Sc<sub>12</sub>}Br<sub>16</sub>Sc, which contain chains of face-sharing square antiprisms and cubes in a ratio of 2:1. Metal–metal bonding is attested by short distances between those endohedral Ir and Os atoms, respectively, which center the square antiprisms (283 pm and 290 pm, respectively). Magnetic and conductivity measurements on {Ir<sub>3</sub>Sc<sub>12</sub>}Br<sub>16</sub> reveal paramagnetism and a small-band-gap semiconductor. This is in accord with electronic structure calculations.

## Introduction

The solid-state chemistry of scandium and gadolinium is dominated by the oxidation state +3 in which, e.g., scandium reaches, as the first transition metal, a noble-gas configuration. There is just one binary scandium halide, the sub-stoichiometric Sc<sub>0.89</sub>I<sub>2</sub><sup>[1]</sup> to which an oxidation state of +2.25 could be allocated. However, this iodide is a metal at high temperatures and an insulator at temperatures below approximately 100 K. With the phase transition upon cooling, the electrons of the 3d band are trapped in localized 3d orbitals such that Sc<sub>0.89</sub>I<sub>2</sub> = Sc<sub>8</sub>I<sub>18</sub> = (Sc<sup>2+</sup>)<sub>6</sub>(Sc<sup>3+</sup>)<sub>2</sub>(I<sup>−</sup>)<sub>18</sub> becomes a mixed-valent compound with clearly addressable

electronic configurations.<sup>[2]</sup> There is more reduced scandium halide chemistry, however. All of these compounds contain octahedral scandium clusters, of which the sesquihalides Sc<sub>2</sub>X<sub>3</sub> (X = Cl, Br) and Sc<sub>7</sub>Cl<sub>10</sub> seem not to require an interstitial atom.<sup>[3]</sup> All the others need a third element to make up for the electron poorness of the third-group element scandium, and of gadolinium as well. These elements can be alkali metals, and there is a small number of ternary halides such as CsSc<sub>1−x</sub>Cl<sub>3</sub>, which crystallize with the so-called hexagonal perovskite type of structure (CsNiCl<sub>3</sub>, BaNiO<sub>3</sub>).<sup>[4]</sup> The electron-donating elements can also be main-group elements like boron, nitrogen, or carbon as well as transition metals like iron, cobalt or nickel, for example. The formula type {ZR<sub>6</sub>}X<sub>12</sub>R<sup>[5]</sup> is especially capable to encapsulate single atoms of all these elements in an octahedral cluster of R atoms (R = Sc, Y, La, Pr, Gd, Tb, Dy, Ho, Er) with the seventh R atom residing in an octahedral void of halogenido ligands contributing their three electrons for intra-cluster bonding.<sup>[6]</sup> In the system C/Sc/I, {CSc<sub>6</sub>}I<sub>12</sub>Sc appears to be the most stable compound; it can be produced in large quantities.<sup>[7]</sup> Except for this iodide with isolated although halide-bridged cluster complexes, {CSc<sub>6</sub>}I<sub>6</sub>I<sup>−a</sup><sub>6/2</sub>I<sup>a−i</sup><sub>6/2</sub>Sc, there are edge-connected chains as in {C<sub>2</sub>Sc<sub>4</sub>}I<sub>6</sub> (with a C<sub>2</sub> unit residing in the cluster)<sup>[8]</sup> and the oligomeric supertetrahedral {Sc<sub>4</sub>C<sub>10</sub>Sc<sub>20</sub>}I<sub>30</sub> (with 10 carbon atoms filling tetrahedral voids in the T3-Sc<sub>20</sub> supertetrahedron).<sup>[9]</sup>

Transition metals have also been explored as endohedral atoms for rare-earth metal clusters and resulted not only in

[a] Department für Chemie, Institut für Anorganische Chemie, Universität zu Köln, Greinstraße 6, 50939 Köln, Germany  
Fax: +49-221-470-5083  
E-mail: gerd.meyer@uni-koeln.de

[b] Institut für Anorganische Chemie und Analytische Chemie, Johannes-Gutenberg-Universität Mainz, Staudinger Weg 9, 55099 Mainz, Germany  
Fax: +49-6131-39-26267  
E-mail: felser@uni-mainz.de

[c] II. Physikalisches Institut, Universität zu Köln, Zùlpicher Straße 77, 50937 Köln, Germany  
Fax: +49-221-470-6708  
E-mail: lorenz@ph2.uni-koeln.de

[d] Fakultät für Chemie, Anorganische Chemie I – Festkörperchemie und Materialien, Ruhr-Universität Bochum, 44780 Bochum, Germany  
Fax: +49-234-32-14951  
E-mail: anja.mudring@rub.de

Supporting information for this article is available on the WWW under <http://dx.doi.org/10.1002/ejic.201000223>.

the  $\{ZR_6\}X_{12}R$ -type stoichiometry but also in the detection of a series of oligomers, which contain the cluster complex  $\{Z_4R_{16}\}X_{36}$ . In this, four  $R_6$  octahedra encapsulating a  $Z$  atom each are connected by common edges. The four  $Z$  atoms form topologically a tetrahedron, but there are little, if any,  $Z$ - $Z$  bonding interactions. These cluster complexes can either be connected by halide bridges yielding the composition  $\{Fe_4Sc_{16}\}X_{20}$  ( $X = Cl, Br$ ),<sup>[10]</sup> or incorporate an additional  $\{Sc_4\}$  tetrahedron with the composition  $\{Z_4Sc_{16}\}Br_{28}\{Sc_4\}$  ( $Z = Mn, Fe, Ru, Os$ ),<sup>[10b]</sup> or additional scandium and chloride to  $\{Z_4Sc_{16}\}Cl_{36}Sc_4$  ( $X = Ru, Os, Ir$ ).<sup>[11]</sup>

Although even the large osmium and iridium atoms may act as endohedral atoms in octahedral clusters in these oligomers, i.e. with coordination number six, it is surprising that they, together with rhenium, may also expand the coordination environment to a coordination number of eight. This is the case in  $\{ReGd_4\}Br_4$ ,  $\{OsSc_4\}Cl_4$ ,  $\{Ir_3Sc_{12}\}Br_{16}$  and  $\{Os_3Sc_{12}\}Br_{16}Sc$ , compounds on which we report here.

## Results and Discussion

Three new reduced scandium halides,  $\{OsSc_4\}Cl_4$ ,  $\{Ir_3Sc_{12}\}Br_{16}$ , and  $\{Os_3Sc_{12}\}Br_{16}Sc$ , with endohedral osmium and iridium atoms, respectively, have been obtained by conproportionation reactions of scandium trihalide,  $ScX_3$  ( $X = Cl, Br$ ), scandium metal and several transition metals at elevated temperatures in sealed tantalum containers.<sup>[10d]</sup> Analogous explorative research with other rare-earth elements, whose standard electrode potentials  $E^\circ$  for the half cells  $R^{2+}/R^{3+}$  are strongly negative, i.e., Y, La, Ce, Pr, Gd, Tb, Dy, Ho, Er, Lu,<sup>[12]</sup> led, among others, to the compound  $\{ReGd_4\}Br_4$  with a crystal structure very similar to that of  $\{OsSc_4\}Cl_4$ .

All formulae of cluster complexes are written in a way that the endohedral atom (Re, Os, Ir) is understood as the central atom (analogous to the central atom of a Werner-type complex), surrounded by a cluster of metal atoms (ligands in Werner-type complexes). The cluster as put in waved brackets is surrounded by halide ions, which complete the cluster complex.<sup>[5]</sup> In  $\{Os_3Sc_{12}\}Br_{16}Sc$  an additional scandium atom resides in an octahedral void composed of bromide ions; it therefore constitutes a coordination sphere of its own. The crystal structure of  $\{OsSc_4\}Cl_4$  is the same as observed for  $\{OsR_4\}Br_4$  ( $R = Y, Er$ )<sup>[13]</sup> and similar to that of the isoelectronic compound  $\{SiTa_4\}Te_4$ .<sup>[14]</sup>  $\{ReGd_4\}Br_4$  crystallizes with a higher symmetry variant of  $\{OsR_4\}X_4$ , space groups  $P4/ncc$  versus  $C2/c$ . The crystal structures of  $\{Ir_3Sc_{12}\}Br_{16}$  and  $\{Os_3Sc_{12}\}Br_{16}Sc$  are new, although they bear strong resemblance to  $\{Ru_3Sc_{12}\}Te_8Sc_{2-x}$ <sup>[15]</sup> and to the afore-mentioned structures.

## Crystal Structures

In all four structures, the transition metal atoms  $Z$ , rhenium, osmium and iridium, respectively, are encapsulated

by a polyhedral cluster of eight scandium/gadolinium atoms, square antiprism and cube, respectively.

In  $\{OsSc_4\}Cl_4$ , there are only square antiprisms present, which are connected by opposite square faces to chains,  $\{OsSc_{8/2}\}$ , running parallel to the crystallographic  $c$  axis of the pseudo-tetragonal  $C$ -centered unit cell (see Figure 1). The triangular faces are capped, and the chains are held together by  $i$ - $a$  connections such that the cluster complex may be written as a whole as  $\{OsSc_{8/2}\}Cl^{i-a}_{4/2}Cl^{a-i}_{(8/2)/2}$ . These “bonds” seem to be stronger than in  $\{SiTa_4\}Te_4$  where no connections between the chains have been claimed. Therefore,  $\{OsSc_4\}Cl_4$  forms rather robust crystals. The Sc–Sc distances are shorter within the square planes (318 pm) than between them, over 350 pm (see Table 1). Os–Sc distances are much shorter, around 270 pm, and this is where the intra-cluster bonding takes place. The Os atoms

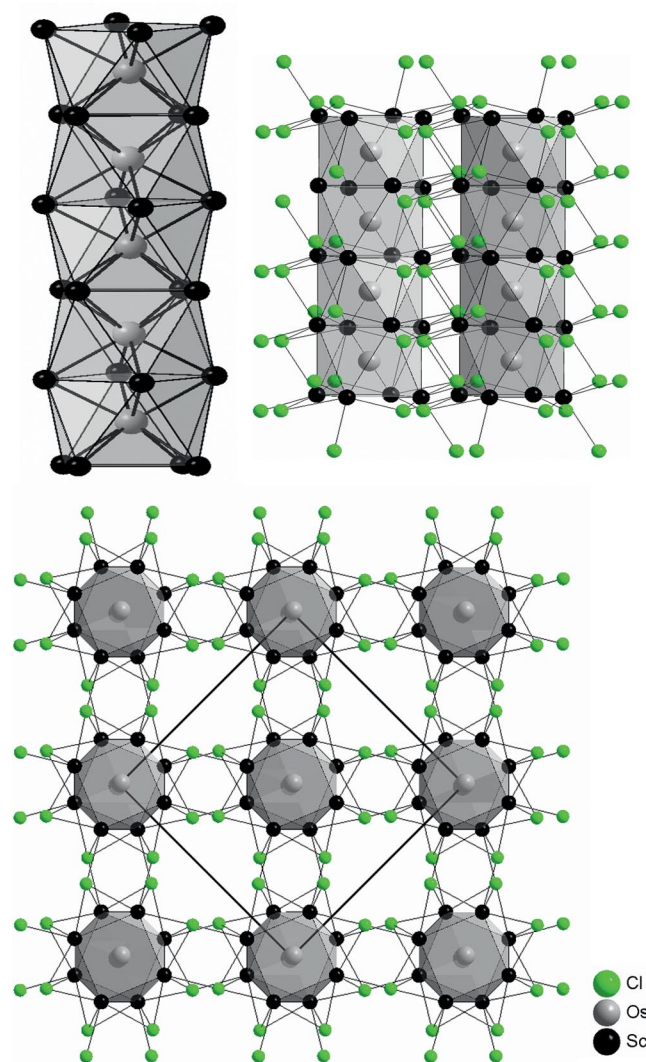


Figure 1. Crystal structure of  $\{OsSc_4\}Cl_4$ . Top left: Chain of face-sharing square antiprisms of scandium atoms with endohedral osmium atoms emphasizing Os–Sc bonding. Top right: View of two parallel chains and their connection by chlorido ligands. Bottom: View from the top onto (001) exhibiting the chains and their connections.

form a chain, but lie surprisingly not on a straight line, the Os–Os–Os angle is 173°. This could be a packing effect. However, in  $\{\text{OsY}_4\}\text{Br}_4$  the same phenomenon is observed, with an angle of 175°.

Table 1. Selected distances and angles for  $\{\text{OsSc}_4\}\text{Cl}_4$  and  $\{\text{ReGd}_4\}\text{Br}_4$ ; Z = Os, Re; R = Sc, Gd; X = Cl, Br.

	$\{\text{OsSc}_4\}\text{Cl}_4$	$\{\text{ReGd}_4\}\text{Br}_4$
Z–Z	307.4	329.3
Z–R	268.8–275.7	291.4 (4×), 297.8 (4×)
	$\langle d \rangle = 272.2$	$\langle d \rangle = 294.4$
R–R	317.6 <sup>[a]</sup> –364.2 <sup>[b]</sup>	345.6 <sup>[a]</sup> (2×), 365.6–385.4 <sup>[b]</sup>
	$\langle d \rangle = 340.4$	$\langle d \rangle = 367.7$
R–X	268.9–278.4	297.1–313.8
	$\langle d \rangle = 273.4$	$\langle d \rangle = 307.3$
X–X <sub>min</sub>	325.1	361.2
Z–Z–Z	173.1	180.0

[a] Within the rectangular faces. [b] Within the triangular faces.

The crystal structure of  $\{\text{ReGd}_4\}\text{Br}_4$  is very similar, isostructural but not isotopic. It crystallizes in the tetragonal space group  $P4/ncc$ , whereas all the others of that formula type crystallize in the monoclinic space group  $C2/c$ . A comparison of the lattice constants of  $\{\text{OsY}_4\}\text{Br}_4$  and  $\{\text{ReGd}_4\}\text{Br}_4$ , which have similar cell volumes [ $1017.3$  vs.  $1061.5(2) \times 10^6 \text{ pm}^3$ ] shows that the former is indeed pseudo-tetragonal by size of the unit cell:

$\{\text{OsY}_4\}\text{Br}_4$ :  $a = 1251.4(5)$ ,  $b = 1238.1(4)$ ,  $c = 656.7(2) \text{ pm}$ ,  $\beta = 90.96(3)^\circ$

$\{\text{ReGd}_4\}\text{Br}_4$ :  $a = b = 1269.56(12)$ ,  $c = 658.59(6) \text{ pm}$

Single crystals of  $\{\text{Ir}_3\text{Sc}_{12}\}\text{Br}_{16}$  grow as very thin needles, which makes the selection of a good crystal rather tedious. Again, there are chains, but the chains now consist of square antiprisms and cubes in a 2:1 ratio (see Figure 2). The iridium atoms centering the polyhedra form a straight line [ $\text{Ir}2\text{--Ir}2\text{--Ir}1$  179.46(3)°,  $\text{Ir}2\text{--Ir}1\text{--Ir}2$  180.00°], although not required by symmetry. However, in contrast to  $\{\text{OsSc}_4\}\text{Cl}_4$  there are now short and long Ir–Ir distances. Those between the centers of the square antiprisms are short (283 pm), and those to the cube centers are long (303 pm). An Ir–Ir bond can be associated with the short distance. The total number of electrons per formula unit of  $\{\text{Ir}_3\text{Sc}_{12}\}\text{Br}_{16}$ , which is available for intra-cluster bonding, is 47. If we subtract two electrons for an Ir–Ir bond, there are 45 left, or 15, scaled per endohedral atom. This is one electron less than for  $\{\text{OsSc}_4\}\text{Cl}_4$  and the same as for  $\{\text{ReGd}_4\}\text{Br}_4$ . The remainder of the structure of  $\{\text{Ir}_3\text{Sc}_{12}\}\text{Br}_{16}$  exhibits rather uniform Sc–Sc distances within the cube (321.2 pm and 323.7 pm) and the same scattering of distances for those within the square antiprisms (see Table 2). The chains are surrounded by bromido ligands, which cap triangular faces of the square antiprisms and edges of the cubes. There is no significant connection between the chains; the shortest interchain Sc–Br distances are 433.5 pm and 441.4 pm. This makes the extreme needle-like growth of the crystals understandable.

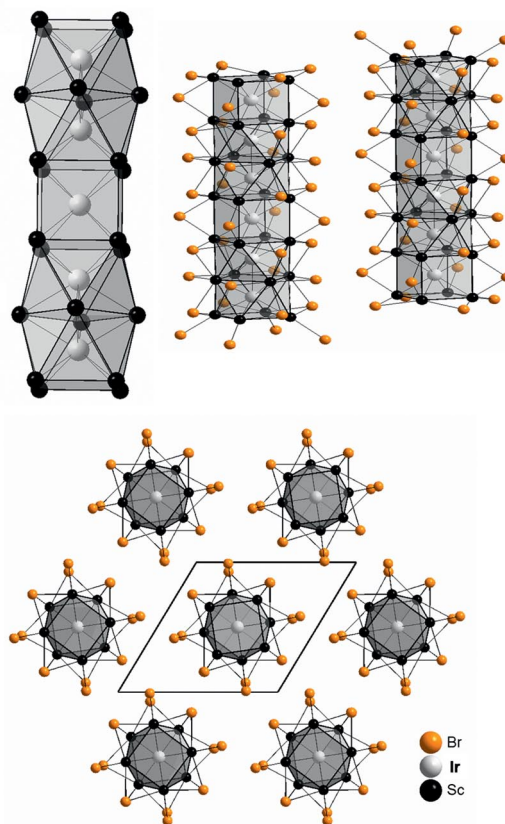


Figure 2. Crystal structure of  $\{\text{Ir}_3\text{Sc}_{12}\}\text{Br}_{16}$ . Top left: Chain of face-sharing square antiprisms and cubes of scandium atoms with endohedral iridium atoms. Top right: View of two parallel chains with apparently no connections by bromido ligands. Bottom: View from the top onto the chains and their arrangement.

Table 2. Selected distances and angles for  $\{\text{Ir}_3\text{Sc}_{12}\}\text{Br}_{16}$  and  $\{\text{Os}_3\text{Sc}_{12}\}\text{Br}_{16}\text{Sc}$ .

	$\{\text{Ir}_3\text{Sc}_{12}\}\text{Br}_{16}$	$\{\text{Os}_3\text{Sc}_{12}\}\text{Br}_{16}\text{Sc}$
Z–Z	283.3, 302.7	290.2, 302.7
Z–R	269.2–280.1	265.0–278.6
	$\langle d \rangle = 275.4$	$\langle d \rangle = 271.9$
R–R	321.2 <sup>[a]</sup> –336.1 <sup>[b]</sup>	316.2 <sup>[a]</sup> –336.9 <sup>[b]</sup>
	$\langle d \rangle = 329.6$	$\langle d \rangle = 330.0$
R–X	264.4–331.1	265.5–328.3
	$\langle d \rangle = 282.6$	$\langle d \rangle = 282.7$
X–X <sub>min</sub>	359.0	361.3
Z–Z–Z	179.5, 180.0	180.0

[a] Within the rectangular faces. [b] Within the triangular faces.

A similar bromide,  $\{\text{Os}_3\text{Sc}_{12}\}\text{Br}_{16}\text{Sc}$ , was obtained with osmium as the endohedral atom. It has the same number of 47 electrons, and the  $\{\text{Os}_3\text{Sc}_{12}\}$  chains are practically the same (see Figure 3). The additional scandium atom is needed to make up for the three electrons less provided by the three endohedral osmium atoms per  $\{\text{Os}_3\text{Sc}_{12}\}$  unit. Intra-chain Os–Os distances are 290 and 303 pm, respectively. The additional scandium atom resides in octahedral voids built up by bromide ions and thereby connects the chains. Although crystal-structure solution and refinement were successful for  $\{\text{Ir}_3\text{Sc}_{12}\}\text{Br}_{16}$  in the small triclinic unit cell as

reported in the Experimental Section, a larger unit cell with  $Z = 2$  may be chosen for better comparison with  $\{\text{Os}_3\text{Sc}_{12}\}\text{Br}_{16}\text{Sc}$  (see Figure 3). Comparable lattice constants are listed in Table 3.

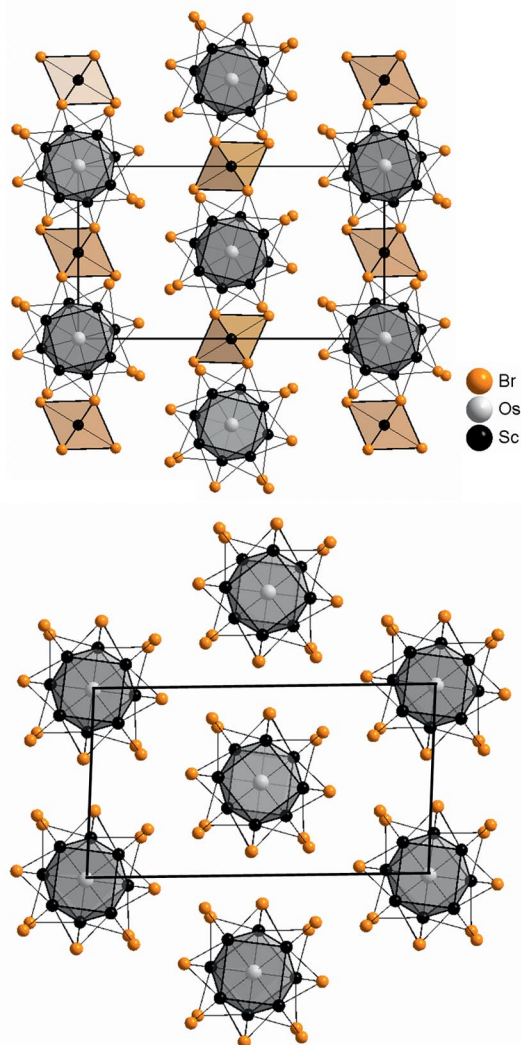


Figure 3. Comparison of the crystal structures of  $\{\text{Os}_3\text{Sc}_{12}\}\text{Br}_{16}\text{Sc}$  (top, with  $[\text{ScBr}_6]$  octahedra emphasized by orange colour) and  $\{\text{Ir}_3\text{Sc}_{12}\}\text{Br}_{16}$  (bottom; with a unit cell of twice the volume, for better comparison); projections onto (001) and (100), respectively.

Table 3. Lattice constants.

$\{\text{Ir}_3\text{Sc}_{12}\}\text{Br}_{16}$	$\{\text{Os}_3\text{Sc}_{12}\}\text{Br}_{16}\text{Sc}$
triclinic, $P\bar{1}$ , $Z = 2$	orthorhombic, $Pnmm$ , $Z = 2$
$b = 1139.9(2)$ pm	$a = 1058.1(2)$ pm
$c = 1864.6(3)$ pm	$b = 1880.4(3)$ pm
$a = 888.6(1)$ pm	$c = 895.5(1)$ pm
$\alpha = 93.14(2)^\circ$	
$\beta = 90.50(2)^\circ$	
$\gamma = 112.64(2)^\circ$	
$V = 1740.0(6) \times 10^6$ pm <sup>3</sup>	$V = 1781.7(4) \times 10^6$ pm <sup>3</sup>

The main structural motif of the crystal structures of  $\{\text{Ir}_3\text{Sc}_{12}\}\text{Br}_{16}$  and  $\{\text{Os}_3\text{Sc}_{12}\}\text{Br}_{16}\text{Sc}$  was also seen for  $\{\text{Z}_3\text{Sc}_{12}\}\text{Te}_8\text{Sc}_{2-x}$ .<sup>[15]</sup> These structures were refined with

$Z = \text{Ru}$  to  $x = 0.79$  and for  $Z = \text{Os}$  to  $x = 0.18$ . This leads to electron counts of 15.9 and 16.5, respectively. For  $x = 1$ , we would have the same number of electrons as in the two above-mentioned bromides.

### Physical Properties: Electrical Conductivity and Magnetic Susceptibility

Electrical conductivity of  $\{\text{Ir}_3\text{Sc}_{12}\}\text{Br}_{16}$  was measured on powder samples of selected and ground single crystals and on single crystals along the needle axis, which is parallel to the cluster chains. As shown in Figure 4, the resistivity of  $\{\text{Ir}_3\text{Sc}_{12}\}\text{Br}_{16}$  shows an activated behavior with an energy gap of approximately 86 meV, which corresponds to an optical band gap of  $2 \times 86$  meV (the pressed powder pellets yield a band gap of about 65 meV). The magnetic susceptibility shows a Curie-like increase at lowest temperatures followed by an almost temperature-independent susceptibility of roughly 0.014 emu/mol above about 100 K. The origin of the paramagnetic susceptibility is unclear at present. One may, however, speculate that it is related to a van Vleck contribution.

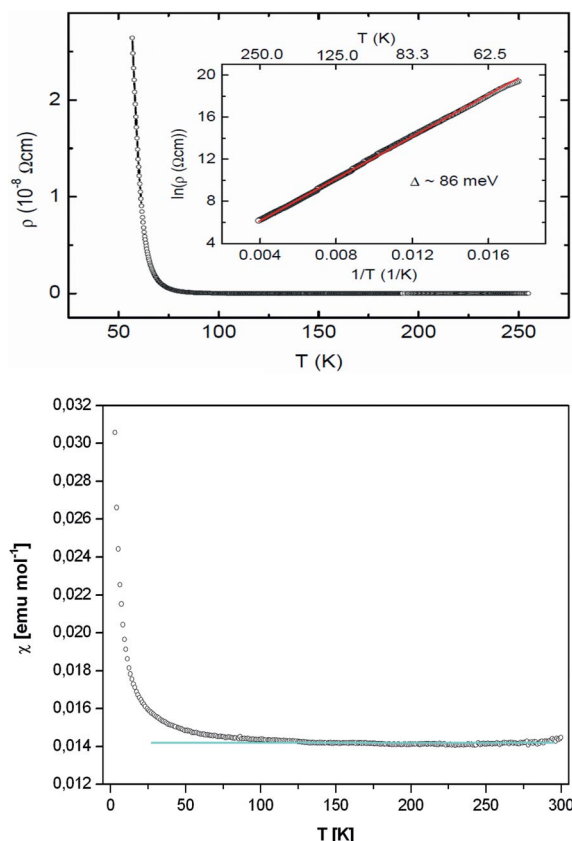


Figure 4. Electrical conductivity along the chain of  $\{\text{Ir}_3\text{Sc}_{12}\}\text{Br}_{16}$  (top). Magnetic susceptibility versus temperature for  $\{\text{Ir}_3\text{Sc}_{12}\}\text{Br}_{16}$  (bottom).

### Electronic Structure

The calculation of the electronic structure for  $\{\text{Ir}_3\text{Sc}_{12}\}\text{Br}_{16}$  (see Supporting Information) predicts a direct

band gap of  $2 \times 86$  meV and in indirect band gap of 71 meV, which is in good agreement with the physical measurements. Analysis of the density of states in  $\{\text{Ir}_3\text{Sc}_{12}\}\text{Br}_{16}$  reveals that the Br energy levels are spread out from  $-5.5$  eV up to the Fermi level, although their contribution to the total density of states is larger at lower energies. The scandium levels are located at quite low energies (the maximum density of states is concentrated around  $-5$  eV). Also the Ir states are found well below the Fermi level. The center of gravity is found at around  $-2$  eV for Ir1 and at around  $-3$  eV for Ir2 with some contribution close to the Fermi level.

The bonding situation in  $\{\text{Ir}_3\text{Sc}_{12}\}\text{Br}_{16}$  was further examined by a crystal orbital Hamiltonian population (COHP) analysis. Bonding is dominated at low energies by Sc–Br interactions, which are strongly bonding but become anti-bonding in character just below the Fermi level. At these energies Ir–Sc bonding interactions become important and over-compensate the anti-bonding contributions to the total energy for  $\{\text{Ir}_3\text{Sc}_{12}\}\text{Br}_{16}$ . In fact, they deliver the major part to the total energy of  $\{\text{Ir}_3\text{Sc}_{12}\}\text{Br}_{16}$ . The Ir–Ir interactions are ambivalent and turn from bonding to anti-bonding and back several times. The integrated COHP values (in eV/cell) show Ir1–Ir2 interactions to be anti-bonding ( $-2.0$ ), whereas a weak attractive interaction exists between Ir2–Ir2 ( $0.2$ ). However, in total the ICOHP for Ir–Ir interactions is negative ( $-1.8$ ). Attractive Sc–Sc interactions come into play just below the Fermi level (ICOHP =  $0.9$  eV/cell). Attractive Sc–Sc bonding can also be found above the Fermi level. However, as can be seen from Figure 5 all other interactions become anti-bonding above the Fermi level. In summary, bonding is optimized in  $\{\text{Ir}_3\text{Sc}_{12}\}\text{Br}_{16}$  by dominating Sc–Br and Ir–Sc interactions.

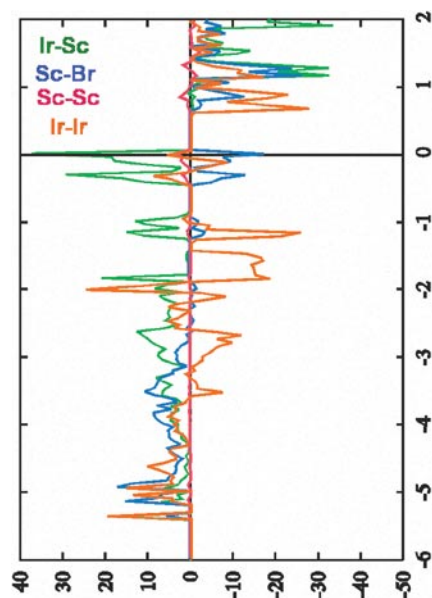


Figure 5. COHP analysis for  $\{\text{Ir}_3\text{Sc}_{12}\}\text{Br}_{16}$ .

Calculation of the electronic structure for  $\{\text{OsSc}_4\}\text{Cl}_4$  reveals strong similarities with that of  $\{\text{Ir}_3\text{Sc}_{12}\}\text{Br}_{16}$ . The band structure shows for  $\{\text{OsSc}_4\}\text{Cl}_4$  also a small band gap

(Supporting Information). Graphical representations of the total density of states and atom-projected densities of states can be found in the Supporting Information. It is obvious from the respective COHP curves that bonding in  $\{\text{OsSc}_4\}\text{Cl}_4$  is, just as in  $\{\text{Ir}_3\text{Sc}_{12}\}\text{Br}_{16}$ , dominated at low energies by attractive Os–Sc interactions, which are strongly bonding but become anti-bonding in character above the Fermi level (see Figure 6). Attractive Sc–Cl interactions dominate at low energies but already become anti-bonding well below the Fermi level. In total, Os–Os interactions as well as Sc–Sc interactions give only minor contributions to the total bonding in  $\{\text{OsSc}_4\}\text{Cl}_4$  and Os–Sc bonding dominates.

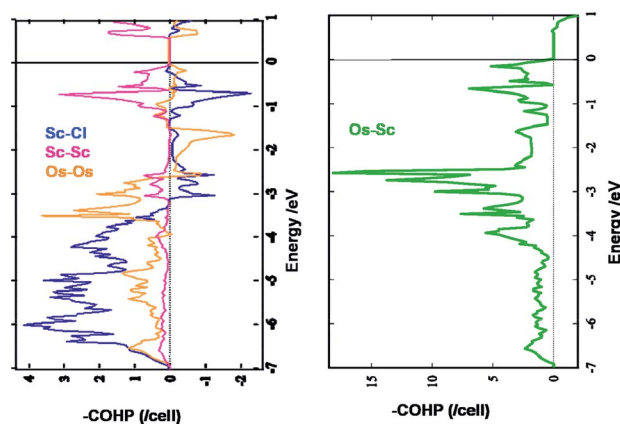


Figure 6. COHP analysis for  $\{\text{OsSc}_4\}\text{Cl}_4$ .

## Conclusions

Four new reduced rare-earth halides with chains of rare-earth element clusters endohedrally stabilized by sixth-period transition metal atoms and surrounded by halogenido ligands were obtained during explorative syntheses in the respective Z/R/X systems. These are  $\{\text{OsSc}_4\}\text{Cl}_4$  and  $\{\text{ReGd}_4\}\text{Br}_4$  with chains of square antiprisms of scandium and gadolinium atoms, respectively, connected by two opposite square faces, and  $\{\text{Ir}_3\text{Sc}_{12}\}\text{Br}_{16}$  and  $\{\text{Os}_3\text{Sc}_{12}\}\text{Br}_{16}$  with square antiprisms and cubes of scandium atoms in a 2:1 ratio, again connected by opposite square faces. Magnetic and electrical conductivity measurements exhibit that  $\{\text{Ir}_3\text{Sc}_{12}\}\text{Br}_{16}$  is a small-band-gap semiconductor. This is in accordance with electronic structure calculations. In all of these compounds, (covalent, polar intermetallic) Z–R and (ionic) R–X bonding is predominant. They are therefore interpreted as (extended, polymeric) anti-Werner cluster complexes according to the formulation, for example,  $\{\text{OsSc}_4\}\text{Cl}_4$ .

## Experimental Section

**Starting Materials:** The rare-earth trihalides  $\text{ScCl}_3$ ,  $\text{ScBr}_3$ , and  $\text{GdBr}_3$  were prepared according to the ammonium halide route<sup>[16]</sup>

from  $\text{Sc}_2\text{O}_3$  and  $\text{Gd}_2\text{O}_3$  (Chempur, 99.9%) and the respective ammonium halides. The crude products were sublimed in high vacuum, stored and handled under inert, especially anhydrous conditions.

**Syntheses and Analyses:** For all syntheses the conproportionation route was used.<sup>[17]</sup> Appropriate amounts of  $\text{RX}_3$ , R metal chips (Aldrich, Chempur) and Z metal powders (Degussa, Düsseldorf; Umicore, Hanau; Merck, Darmstadt) were weighed within a dry-box (MBraun, Garching, Germany) with water and oxygen levels of <1 ppm in tantalum tubes of about 5 cm length, which were pre-cleaned, crimped and sealed at one side. After sealing the other side by He arc-welding, the tantalum ampoules were jacketed with silica ampoules. These were then transferred to a furnace. After the reactions were completed, the silica jacket was removed, and the tantalum ampoules were opened in the dry box and their contents inspected with the aid of a microscope. Single crystals were selected, transferred to thin-walled glass capillaries and sealed with a hot wire. Powder X-ray diffraction patterns were recorded with representative samples of the bulk materials with a Stoe Stadi P diffractometer (Mo- $K_\alpha$  radiation) to confirm the purity of the reaction products. Further analyses like elemental analyses were not undertaken as they would only have confirmed the element ratios weighed into the tantalum ampoules. EDX measurements were performed in some cases on single crystals and always confirmed the element ratios as determined by single-crystal X-ray structure determinations. Stoichiometries, temperature programs and products for the respective reactions under consideration here were as follows.

**{OsSc<sub>4</sub>}Cl<sub>4</sub>:** 100 mg (0.66 mmol)  $\text{ScCl}_3$ , 60 mg (1.33 mmol) Sc, 94 mg (0.5 mmol) Os; heat from ambient temperature quickly to 500 °C, then further to 1200 °C, hold there for 72 h and cool with 5 °C/h to ambient temperature. Long and thin, black shiny needles often attached to colorless plates of  $\text{ScOCl}$ .

**{ReGd<sub>4</sub>}Br<sub>4</sub>:** 150 mg (0.38 mmol)  $\text{GdBr}_3$ , 71 mg (0.45 mmol) Gd, 42 mg (0.23 mmol) Re; heat from ambient temperature quickly to 880 °C, hold there for 24 h and cool with 2 °C/h to 830 °C, anneal for 16 d and cool rapidly to ambient temperature with an ice bath. Black shiny cuboids of rectangular shape.

**{Ir<sub>3</sub>Sc<sub>12</sub>}Br<sub>16</sub>:** 200 mg (0.7 mmol)  $\text{ScBr}_3$ , 40 mg (0.88 mmol, excess) Sc, 57 mg (0.3 mmol) Ir; heat from ambient temperature to 925 °C, hold there for two weeks, cool with 2 °C/h to 500 °C and then quench. Long and thin black needles in company of violet  $\text{ScOBr}$ .

**{Os<sub>3</sub>Sc<sub>12</sub>}Br<sub>16</sub>Sc:** 200 mg (0.7 mmol)  $\text{ScBr}_3$ , 63 mg (1.4 mmol) Sc, 100 mg (0.52 mmol) Os; heat rapidly to 1100 °C, hold there for 2 d and cool with 5 °C/h to room temperature. Long, stable black shiny needles accompanied by violet  $\text{ScOBr}$ .

Single crystals of the respective halides as selected under the microscope in the dry box were inspected by Laue photographs (Mo- $K_\alpha$  radiation, image plate). The best specimen was transferred to a Stoe "Image Plate Diffraction System" (IPDS-I and -II), and complete data sets were recorded. The data were corrected for Lorentz and polarization effects. A numerical absorption correction based on crystal-shape optimization was applied for all data. The programs used in this work are Stoe's X-Area, including X-RED and X-Shape for data reduction and absorption correction, and the programs X-Step, including SIR-92, SHELXS-97 and SHELXL-97 for structure solution and refinement.<sup>[18]</sup> The last cycles of refinement included atomic positions and anisotropic thermal parameters for all atoms. Further details on the crystal structure investigations may be obtained from the Fachinformationszentrum Karlsruhe, 76344 Eggenstein-Leopoldshafen, Germany (Fax: +49-7247-808-

666; E-mail: crysdata@fiz-karlsruhe.de), on quoting the depository numbers CSD-421532 (for {OsSc<sub>4</sub>}Cl<sub>4</sub>), -421534 (for {ReGd<sub>4</sub>}Br<sub>4</sub>), -421533 (for {Ir<sub>3</sub>Sc<sub>12</sub>}Br<sub>16</sub>), and -421535 (for {Os<sub>3</sub>Sc<sub>12</sub>}Br<sub>16</sub>Sc).

#### Crystal Data and Structure Refinements

**{OsSc<sub>4</sub>}Cl<sub>4</sub>:** Monoclinic, space group  $C2/c$  (No. 15);  $a = 1131.1(3)$  pm,  $b = 1130.1(3)$  pm,  $c = 613.6(1)$  pm,  $\beta = 90.44(2)^\circ$ ,  $V = 784.3(3) \times 10^6$  pm<sup>3</sup>;  $Z = 4$ ;  $3.60^\circ < \theta < 27.74^\circ$ ; Mo- $K_\alpha$  radiation (graphite monochromator,  $\lambda = 71.073$  pm);  $F(000) = 912$ ;  $\mu = 20.682$  mm<sup>-1</sup>; 3218 reflections measured, 847 unique, 831 observed.  $R_{\text{int}} = 0.1349$ ,  $R1/wR2 = 0.1314/0.2691$  [ $I_0 > 2\sigma(I_0)$ ] and 0.1323/0.2696 (all data); goodness-of-fit on  $F^2 = 1.353$ .

**{ReGd<sub>4</sub>}Br<sub>4</sub>:** Tetragonal, space group  $P4/ncc$  (No. 130);  $a = 1269.56(12)$  pm,  $c = 658.59(6)$ ,  $V = 1061.50(17) \times 10^6$  pm<sup>3</sup>;  $Z = 4$ ;  $2.27^\circ < \theta < 29.57^\circ$ ; Mo- $K_\alpha$  radiation (graphite monochromator,  $\lambda = 71.073$  pm);  $F(000) = 1884$ ;  $\mu = 50.984$  mm<sup>-1</sup>; 9847 reflections measured, 751 unique, 635 observed.  $R_{\text{int}} = 0.0713$ ,  $R1/wR2 = 0.0301/0.0770$  [ $I_0 > 2\sigma(I_0)$ ] and 0.0363/0.0796 (all data); goodness-of-fit on  $F^2 = 1.062$ .

**{Ir<sub>3</sub>Sc<sub>12</sub>}Br<sub>16</sub>:** Triclinic, space group  $P\bar{1}$  (No. 2);  $a = 888.7(2)$  pm,  $b = 1063.7(2)$  pm,  $c = 1123.4(2)$  pm,  $\alpha = 116.96(1)^\circ$ ,  $\beta = 102.02(1)^\circ$ ,  $\gamma = 101.75(1)^\circ$ ,  $V = 870.0(3) \times 10^6$  pm<sup>3</sup>;  $Z = 1$ ;  $2.49^\circ < \theta < 28.03^\circ$ ; Mo- $K_\alpha$  radiation (graphite monochromator,  $\lambda = 71.073$  pm);  $F(000) = 1043$ ;  $\mu = 31.955$  mm<sup>-1</sup>; 7518 reflections measured, 3839 unique, 3062 observed.  $R_{\text{int}} = 0.0560$ ,  $R1/wR2 = 0.0572/0.1492$  [ $I_0 > 2\sigma(I_0)$ ] and 0.0693/0.1610 (all data); goodness-of-fit on  $F^2 = 1.054$ .

**{Os<sub>3</sub>Sc<sub>12</sub>}Br<sub>16</sub>Sc:** Orthorhombic, space group  $Pnmm$  (No. 58);  $a = 1058.1(2)$  pm,  $b = 1880.4(3)$  pm,  $c = 895.5(1)$  pm,  $V = 1781.7(4) \times 10^6$  pm<sup>3</sup>;  $Z = 2$ ;  $2.52^\circ < \theta < 28.12^\circ$ ; Mo- $K_\alpha$  radiation (graphite monochromator,  $\lambda = 71.073$  pm);  $F(000) = 2121$ ;  $\mu = 30.878$  mm<sup>-1</sup>; 12371 reflections measured, 2021 unique, 1094 observed.  $R_{\text{int}} = 0.1173$ ,  $R1/wR2 = 0.0644/0.1541$  [ $I_0 > 2\sigma(I_0)$ ] and 0.1081/0.1687 (all data); goodness-of-fit on  $F^2 = 0.866$ .

**Physical Properties:** Magnetic susceptibilities were measured for the example of {Ir<sub>3</sub>Sc<sub>12</sub>}Br<sub>16</sub> with a Quantum Design MPMS XL squid magnetometer in the temperature range between 1.8 and 300 K. Diamagnetic corrections were performed by using Pascal's constants.<sup>[19]</sup> Specific resistivities were measured for pressed powder pellets under strict exclusion of air/water by the conventional four-point method. A needle (actually a conglomerate of thin needles) of {Ir<sub>3</sub>Sc<sub>12</sub>}Br<sub>16</sub> was contacted on both ends such that the specific resistance could be measured along the needle axis, the crystallographic  $a$  axis.

**Computational Details:** In order to analyze the bonding situation and the physical properties, calculations regarding the electronic structure were carried out with the Stuttgart LMTO-ASA program package, which uses the tight-binding linear-muffin-tin orbital (LMTO) method in the local density (LDA) and atomic sphere (ASA) approximation.<sup>[20,21]</sup> All major relativistic effects except spin-orbit coupling were taken into account by using scalar relativistic approximations. The calculations include corrections for the neglect of the interstitial regions and the partial waves of higher order. To reduce the overlap of atomic spheres (AS), empty interstitial spheres were added to the crystal potential and the basis set. The construction of the atomic sphere radii was performed according to an automatic procedure of the program package until the empty space was sufficiently filled.<sup>[22]</sup> In the calculation of the electronic structure of {Ir<sub>3</sub>Sc<sub>12</sub>}Br<sub>16</sub> the basis set of short-ranged, atom-centered TB-LMTOs contained 4s, 5s and 4p for Br. The s waves were included only in the tails of the LMTOs according to the Löwdin downfolding procedure.<sup>[23]</sup> For scandium (iridium) 4s

and 3d (6s, 6p and 5d) functions were taken fully into account, whereas the 4p (4f) functions were downfolded. In the calculation of the electronic structure of  $\{\text{OsSc}_4\}\text{Cl}_4$  scandium (osmium) 4s and 3d (6s, 6p and 5d) functions were taken fully into account, whereas the 4p (4f) functions were downfolded. All reciprocal space integrations were carried out by using the tetrahedron method.<sup>[24]</sup> To examine in detail the effect of the anion on the electronic density of states, the partial-ion  $l$  and  $m$  quantum-number-decomposed electronic density of states has been calculated. They were calculated by projecting the wave functions onto spherical harmonics centered on each atom (PDOS = projected density of states). For bond analysis the crystal orbital Hamiltonian population (COHP) method was used together with its integration, the ICOHP.<sup>[25]</sup> In all cases the structural data were employed as gained from single-crystal X-ray data. The highest occupied level was always chosen as the level of reference for the energy.

**Supporting Information** (see footnote on the first page of this article): Further information on the electronic structures of  $\{\text{OsSc}_4\}\text{Cl}_4$  and  $\{\text{Ir}_3\text{Sc}_{12}\}\text{Br}_{16}$ .

## Acknowledgments

This work has been supported by the State of Nordrhein-Westfalen through the Universities of Cologne and Bochum, especially within the framework of the Sonderforschungsbereich 608 (Complex transition metal compounds with spin and charge degrees of freedom and disorder), supported by the Deutsche Forschungsgemeinschaft, Bonn. A. V. M. is grateful for the Dozentenstipendium awarded by the Fonds der Chemischen Industrie, Frankfurt am Main.

- [1] a) B. C. McCollum, J. D. Corbett, *J. Chem. Soc., Chem. Commun.* **1968**, 1666; b) B. C. McCollum, D. J. Dudis, A. Lachgar, J. D. Corbett, *Inorg. Chem.* **1990**, *29*, 2030.
- [2] G. Meyer, L. Jongen, A.-V. Mudring, A. Möller, *Inorganic Chemistry in Focus* (Eds.: G. Meyer, D. Naumann, L. Wesemann), Wiley-VCH, Weinheim, **2005**, vol. 2, pp. 105–120.
- [3] a) B. C. McCollum, M. J. Camp, J. D. Corbett, *Inorg. Chem.* **1973**, *12*, 778; b) K. R. Poeppelmeier, J. D. Corbett, *Inorg. Chem.* **1977**, *16*, 1107–1111.
- [4] a) K. R. Poeppelmeier, J. D. Corbett, T. P. McMullen, D. R. Torgeson, R. G. Barnes, *Inorg. Chem.* **1980**, *19*, 129; b) J. D. Corbett, G. Meyer, *Inorg. Chem.* **1981**, *20*, 2627.
- [5] This nomenclature for cluster complexes has recently been proposed. It considers cluster complexes as anti-Werner complexes: G. Meyer, *Z. Anorg. Allg. Chem.* **2008**, *634*, 2729.
- [6] a) S. J. Hwu, J. D. Corbett, *J. Solid State Chem.* **1986**, *64*, 331; b) D. S. Dudis, J. D. Corbett, S. J. Hwu, *Inorg. Chem.* **1986**, *25*, 3434; c) T. Hughbanks, J. D. Corbett, *Inorg. Chem.* **1988**, *27*, 2022; d) S. Zimmermann, Dissertation, University of Köln, **2008**; e) M. Brühmann, K. Daub, C. Rustige, G. Meyer, unpublished results.
- [7] S. Demir, Diplomarbeit, University of Köln, **2008**.
- [8] D. S. Dudis, J. D. Corbett, *Inorg. Chem.* **1987**, *26*, 1933.
- [9] L. Jongen, A.-V. Mudring, G. Meyer, *Angew. Chem. Int. Ed.* **2006**, *45*, 1886; *Angew. Chem.* **2006**, *118*, 1920.
- [10] a) M. W. Payne, M. Ebihara, J. D. Corbett, *Angew. Chem. Int. Ed. Engl.* **1991**, *30*, 856; b) S. J. Steinwand, J. D. Corbett, *Inorg. Chem.* **1996**, *35*, 7056; c) S. Zimmermann, G. Meyer, Diplomarbeit, University of Köln, **2006**; d) S. Zimmermann, Dissertation, University of Köln, **2008**.
- [11] a) M. Ebihara, J. D. Martin, J. D. Corbett, *Inorg. Chem.* **1994**, *33*, 2079; b) S. J. Steinwand, J. D. Corbett, J. D. Martin, *Inorg. Chem.* **1997**, *36*, 6413; c) K. Daub, Dissertation, University of Köln, **2009**.
- [12] a) D. A. Johnson, *J. Chem. Soc. A* **1969**, 1525; D. A. Johnson, *J. Chem. Soc. A* **1969**, 1529; D. A. Johnson, *J. Chem. Soc. A* **1969**, 1525; D. A. Johnson, *J. Chem. Soc. A* **1969**, 2578; *Some Thermodynamic Aspects of Inorganic Chemistry*, 2nd ed., Cambridge University Press, **1982**, in: *Inorg. Chem. Focus*, vol. 3 (Eds.: G. Meyer, D. Naumann, L. Wesemann), Wiley-VCH, Weinheim, **2006**, pp. 1–13; b) L. R. Morss, in: *Standard Electrode Potentials in Solution* (Eds.: A. J. Bard, R. Parsons, J. Jordan), Marcel Dekker, New York, **1985**, p. 587; G. Meyer, *Chem. Rev.* **1976**, *76*, 827; c) G. Meyer, *Chem. Rev.* **1988**, *88*, 93–107; d) G. Meyer, *Z. Anorg. Allg. Chem.* **2007**, *633*, 2537–2552.
- [13] P. K. Dorhout, J. D. Corbett, *J. Am. Chem. Soc.* **1992**, *114*, 1697–1701.
- [14] M. E. Badding, F. J. DiSalvo, *Inorg. Chem.* **1990**, *29*, 3952–3954.
- [15] L. Chen, J. D. Corbett, *J. Am. Chem. Soc.* **2003**, *125*, 1170–1171.
- [16] a) G. Meyer, P. Ax, *Mater. Res. Bull.* **1982**, *17*, 1447–1455; b) G. Meyer, S. Dötsch, Th. Staffel, *J. Less-Common Met.* **1987**, *127*, 155–160; c) G. Meyer, *Inorg. Synth.* **1989**, *25*, 146–150; d) G. Meyer, in: *Synthesis of Lanthanide and Actinide Compounds* (Eds.: G. Meyer, L. R. Morss), Kluwer Academic Publishers, Dordrecht, The Netherlands, **1991**, pp. 135–144.
- [17] J. D. Corbett, in: *Synthesis of Lanthanide and Actinide Compounds* (Eds.: G. Meyer, L. R. Morss), Kluwer Academic Publishers, Dordrecht, The Netherlands, **1991**, pp. 159–173.
- [18] *X-Shape 1.06, Crystal Optimisation for Numerical Absorption Correction (C)*, Stoe & Cie GmbH, Darmstadt, **1999**; *X-Area 1.16*, Stoe & Cie GmbH, Darmstadt, **2003**; *X-RED 1.22*, Stoe Data Reduction Program (C), Stoe & Cie GmbH, Darmstadt, **2001**; *X-STEP32*, Revision 1.06f, STOE & Cie GmbH, Darmstadt, **2000**; SIR-92: A. Altomare, G. Cascarano, G. Giacovazzo, *J. Appl. Crystallogr.* **1993**, *26*, 343; G. M. Sheldrick, *SHELXL-97, Programs for Crystal Structure Analysis*, University of Göttingen, **1997**.
- [19] W. Haberditzl, *Magnetochemie*, Akademie-Verlag, Berlin, Germany, **1968**.
- [20] a) H. L. Shriver, *The LMTO Method*, Springer-Verlag, Berlin, Germany, **1984**; b) O. Jepsen, M. Snob, O. K. Andersen, *Linearized Band-Structure Methods in Electronic Band-Structure and Its Applications* (Springer Lecture Note), Springer Verlag, Berlin, Germany, **1987**; c) O. K. Andersen, O. Jepsen, *Phys. Rev. Lett.* **1984**, *53*, 2571.
- [21] R. W. Tank, O. Jepsen, A. Burckhardt, O. K. Andersen, *TB-LMTO-ASA Program*, Vers. 4.7, Max-Planck-Institut für Festkörperforschung, Stuttgart, Germany, **1998**.
- [22] O. Jepsen, O. K. Andersen, *Z. Phys.* **1995**, *B97*, 35.
- [23] W. R. L. Lambrecht, O. K. Andersen, *Phys. Rev. B* **1986**, *34*, 2439; O. Jensen, O. K. Andersen, *Z. Phys. B* **1995**, *97*, 35; G. Krier, O. Jepsen, O. K. Andersen, Max-Planck-Institute für Festkörperforschung, Stuttgart, Germany, unpublished results.
- [24] a) W. R. L. Lambrecht, O. K. Andersen, *Phys. Rev. B* **1986**, *34*, 2439; b) O. Jensen, O. K. Andersen, *Z. Phys. B* **1995**, *97*, 35; c) G. Krier, O. Jepsen, O. K. Andersen, Max-Planck-Institut für Festkörperforschung, Stuttgart, Germany, unpublished results.
- [25] R. Dronskowski, P. E. Blöchl, *J. Phys. Chem.* **1993**, *97*, 8617.

Received: February 25, 2010  
Published Online: May 5, 2010